

Common Sense Reasoning for Deepfake Detection

Yue Zhang¹, Ben Colman², Ali Shahriyari², Gaurav Bharaj²
¹ Michigan State University ² Reality Defender

zhan1624@msu.edu, {ben, ali, gaurav}@realitydefender.ai

Abstract

State-of-the-art approaches rely on image-based features extracted via neural networks for the deepfake detection binary classification. While these approaches trained in the supervised sense extract likely fake features, they may fall short in representing unnatural ‘non-physical’ semantic facial attributes – blurry hairlines, double eyebrows, rigid eye pupils, or unnatural skin shading. However, such facial attributes are generally easily perceived by humans via common sense reasoning. Furthermore, image-based feature extraction methods that provide visual explanation via saliency maps can be hard to be interpreted by humans. To address these challenges, we propose the use of common sense reasoning to model deepfake detection, and extend it to the Deepfake Detection VQA (DD-VQA) task with the aim to model human intuition in explaining the reason behind labeling an image as either real or fake. To this end, we introduce a new dataset that provides answers to the questions related to the authenticity of an image, along with its corresponding explanations. We also propose a Vision and Language Transformer-based framework for the DD-VQA task, incorporating text and image aware feature alignment formulations. Finally, we evaluate our method on both the performance of deepfake detection and the quality of the generated explanations. We hope that this task inspires researchers to explore new avenues for enhancing language-based interpretability and cross-modality applications in the realm of deepfake detection.

1. Introduction

The rise of generative methods [15, 20–22] enables new capabilities to create and manipulate images. While these advances empower human creativity and enable numerous AI-for-good applications [33, 36], they can also be used to create and spread misinformation, potentially leading to social problems and security threats [45, 48, 49]. As a result, with the increasing prevalence of generative media (deepfakes), a growing number of advanced deepfake detection algorithms [6, 19, 34] are being developed to discern

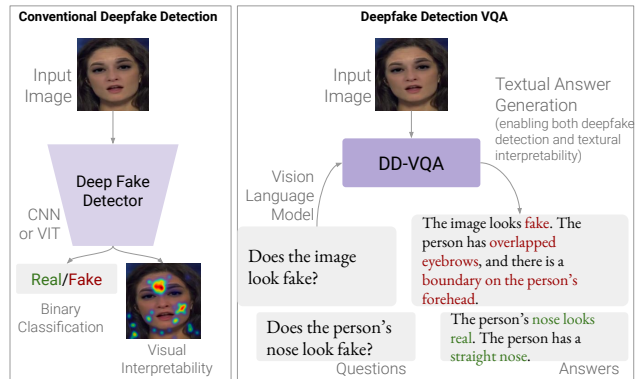


Figure 1. Illustration of the Deepfake Detection VQA (DD-VQA) Task. Traditional methods categorize deepfake detection as a binary classification task. However, we extend the task to a multi-modal task, enabling the generation of real/fake answers and corresponding explanations in response to a given question.

media authenticity and mitigate such serious concerns.

Previous deepfake detection methods primarily function as binary classifiers, including approaches such as convolution neural networks (CNNs) [40], self-blending techniques [40] and diffusion model detection [34]. These methods aim to enhance the model’s interpretability via saliency maps based on visual features [12, 13, 39]. However, providing detailed explanations for the underlying reasons of authenticity or fakeness, especially in the form of explicit text explanations, remains an area with limited exploration. In fact, answering the question of “Why the image is a deepfake?” is a greater challenge than “Whether the image is a deepfake?”. The former requires reasoning and common-sense knowledge that is not explicit in images. We acknowledge that certain deepfake models can now generate images that effectively deceive individuals [29]; however, we draw inspiration from the concept of the *uncanny valley* [14], where humans occasionally experience discomfort (eeriness) for hallucinated human images that appear almost, but not quite *human-like*. Here, humans utilize common-sense knowledge [24, 47], especially for semantically meaningful facial attributes (e.g. non-physical facial components or unnatural skin shading), to explain “what’s wrong” in an

image, while current deepfake detection classifiers methods lack such an ability explicitly.

To address the above challenge, we introduce an approach that extends the deepfake detection from a binary classification task to a generative visual question-answering task, named **Deepfake Detection Visual Question Answer (DD-VQA)** task (see Fig. 1). In this task, the objective is to generate answers based on questions and images, where the answers are not limited to providing deepfake detection results but also to describe the corresponding textual explanations grounded in common-sense knowledge. Unlike previous methods that solely offer a general assessment of the entire facial authenticity, we provide fine-grained questions to assess the authenticity of facial components, including *skin, eyebrows, eyes, nose, and mouth*. For instance, in the example of Fig. 1, the person’s *overlapped eyebrows* is an obvious indicator of fakeness, whereas the person’s *naturally straight nose* appears relatively realistic.

While this research direction is compelling, no dataset is currently available for this task. To enable research in this area, we introduce a novel dataset, named DD-VQA dataset, that includes the triplets – image, question and answers. The images in the DD-VQA dataset are sourced from the FaceForensics++ (FF++) dataset [35]. We design general and fine-grained questions for each image to inquire about the authenticity of the entire image and facial components. The answers are collected from annotators, who provide both real/fake decisions and corresponding reasons based on their common-sense knowledge.

DD-VQA task is challenging since, besides understanding the question and image, the model needs to (1) determine the authenticity of the individual facial component based on the questions asked and (2) learn common-sense knowledge to generate reasonable textual explanations. We observe that the prevailing large Vision-Language (VL) pre-trained models [2, 25, 55] encounter limitations on the DD-VQA task (see Fig. 5). Such pre-trained VL models tend to provide generic descriptions of facial features and often fall short when distinguishing image authenticity while offering reasonable explanations. Therefore, we fine-tune a pre-trained VL model with the DD-VQA dataset as our proposed benchmark. Additionally, we design text and image contrastive losses to enhance the model’s representation learning for the deepfake detection task.

To summarize, our contributions are:

1. We introduce a novel DD-VQA task and the corresponding dataset enabling the generation of detection decisions along with textual explanations based on common-sense knowledge.¹
2. We provide a multi-modal Transformer model as the benchmark and enhance representation learning for the deepfake detection task with a novel text and image con-

trastive learning formulation.

3. We evaluate the performance of DD-VQA in both aspects of deepfake detection and text generation. We also provide a comprehensive analysis to show that incorporating textual explanation can improve both detection and interpretability of the deepfake detection model.

2. Related Works

Deepfake Detection. Deep learning methods are the dominant approaches for the deepfake detection task. The traditional CNN-based methods such as Xception [7] and EfficientNet [44] have achieved satisfying results in intra-dataset. To improve the generalization ability, Face X-ray [26] identify boundary inconsistencies as a common forgery cue to incorporate domain prior knowledge to encourage the model to learn general forgery features. Some works have explored multi-task learning in deepfake detection task [17, 18]. However, there is very limited research integrating natural language into deepfake datasets or deepfake detection models. VLFFD [42] proposes a visual-linguistic paradigm to use language as supervision to improve deepfake detection, but their text information is automatically generated and only focuses on aspects like manipulation region, type, and method. In our work, we introduce a novel VQA dataset that offers free-form textual explanations regarding the authenticity of the image based on human common-sense knowledge.

Interpretable Deepfake Detection Models. The current methods primarily treat deepfake detection as a binary classification task. The approaches used to interpret deepfake detection models mainly align with the methods used to explain neural network classifiers. The prominent approach uses gradient-based methods [39, 41, 43] to visualize the highlight regions for the prediction. Another line of research attempts to build an interpretable network by model design; for instance, DFGNN [23] applies interpretable GNN to deepfake detection tasks. DPNET [46] propose an interpretable prototype-based neural network that captures dynamic features to explain the prediction. While these methods have been used to enhance the model’s interpretability, describing the reasons for the determination in natural language has yet to be explored extensively. Our work introduces a novel VQA task that generates deepfake detection results and the corresponding textual reasons. To the best of our knowledge, we are the first to enhance the interpretability of deepfake detection models by generating explicit textual explanations.

Vision-Language Learning. Multi-modal learning, especially Vision-Language (VL) learning, has gained significant attention within the AI community. Recently, an increasing number of large VL pre-training models have emerged, such as BLIP [25], Flamingo [2], and MiniGPT4 [55]. These models are all based on the Transformer architecture and have been trained on various VL datasets and tasks. These large

¹The dataset will be released to encourage research in this area.

| # | Facial Features | Fake | Real |
|---|------------------|--|--|
| 1 | Eyebrows | overlapping, broken, blurred, etc. | arched, straight, thick, thin, bushy, sparse, etc. |
| 2 | Skin | boundaries, stain, flaws, inconsistent color, etc. | smooth, illuminated, wrinkled, even, etc. |
| 3 | Eyes | overly large, small, blurred, too rigid, etc. | round, oval, deep, large, small, sparking, etc. |
| 4 | Nose | unnaturally curved, lack of details, no nose, etc. | straight, pointed, broad, etc. |
| 5 | Mouth/Teeth/Chin | overly large, small mouth, unnatural color for mouth, teeth, overly pointed, square chin, etc. | full, thin, pouty mouth, white/aligned/misaligned teeth, overly squared/ pointed chins, etc. |
| 6 | Others | mismatched bangs/ fringe/mustache/beard, blurry eye-glasses frame, inconsistent/unrealistic shadow, etc. | complete face feature, proper hair/bangs/hairstyle, matched mustache/beard, etc. |

Table 1. Annotation vocabulary for the reasons of authenticity or fakeness based on common-sense knowledge.

VL models have achieved remarkably high performance in many applications, such as Visual Question Answering (VQA) [5], Vision and Language Navigation (VLN) [4, 52–54], and Image Captioning [1, 51]. Despite their popularity, relatively little research has been dedicated to examining these models’ performance in deepfake detection. In our research, we apply current Vision-Language (VL) pre-training models to our proposed deepfake detection VQA dataset to explore their capacity for the deepfake detection task.

Visual Question Answering (VQA). VQA has been one of the most popular research topics. The task requires reasoning ability on visual images and textual questions to predict the correct answer. A large-scale VQA dataset with free-form questions created by humans is first proposed in [5]. VQA v2.0 [16] introduces a more balanced dataset by reducing the language biases in the VQA dataset. OK-VQA [38] extends the in-domain VQA task with external knowledge. We are pioneering in extending deepfake detection into the research area of the VQA task. Our VQA task is a generative rather than a classification task to select the best answer from a set of pre-defined answers.

3. Deepfake Detection VQA

Deepfake Detection VQA task is to generate answers given an image and a question to discern facial authenticity. In the following sections, we first present our methods of constructing the DD-VQA dataset in Sec 3.1, and then we introduce our proposed benchmark for this task in Sec 3.2.

3.1. DD-VQA Dataset

To the best of our knowledge, we are the pioneering research utilizing textural common-sense knowledge for the deepfake detection task. Thus, there is no existing dataset that can be directly used for this purpose. We present our methodology on how we construct the DD-VQA dataset.

The manipulated images are collected from the Face-Forensics++ dataset (FF++) [35]. The FF++ dataset, widely used in deepfake research, contains 5,000 videos. Among these, 1,000 videos are real, while 4,000 videos are fake, employing four different manipulation methods: *Deepfakes*, *Face2Face*, *FaceSwap*, and *NeuralTextures*. While we acknowledge the existence of deepfake datasets that are even

more effective at deceiving individuals [29], our goal is to explore the use of text to explain obvious deepfake indicators. For this purpose, we use the FF++ dataset, which is relatively easier to identify and describe manipulation regions. The FF++ dataset solely provides video frames, and our primary focus is to assess the authenticity of the human faces in the image. So, in our initial step, we extract one frame from each video and crop the human face from the frame. The image is sized at 480×480 pixels with complete human faces. After collecting images, we gather the corresponding question-answer pairs based on our designed annotation schemes, as introduced below.

3.1.1 Annotation Scheme

We utilize Amazon Mechanical Turk ² as our annotation platform and assign annotators task of providing answers based on given images and questions. We design two types of questions for each image: **general questions** and **fine-grained questions**. The general question is discerning the authenticity of the person depicted in the image, while the fine-grained questions delve into the authenticity of different facial components (*skin*, *eyes*, and etc.). For both questions, the answers are not only expected binary yes-or-no answers, but also detailed factors based on common-sense knowledge.

Annotation Challenges. After collecting the initial batch of annotations, we observe that annotators struggle to provide detailed descriptions of the characteristics of authenticity or fakeness. For example, a large portion of annotations contain only detection results, leaving the explanation part blank. Even when explanations are provided, annotators tend to use very general terms, such as “*unrealistic skin*” or “*unnatural eyebrow*”. To address this issue, we design a set of predefined reasons based on human common-sense knowledge. We list some descriptive expressions to specify the reasons for the authenticity and fakeness of different facial components in Tab 1. These expressions are formulated as multiple-choice lists for annotators to select when responding to each question. Additionally, annotators maintain the flexibility to provide additional explanations, contributing to refining our answer lists.

General Questions assess the overall authenticity of an im-

²<https://www.mturk.com/>

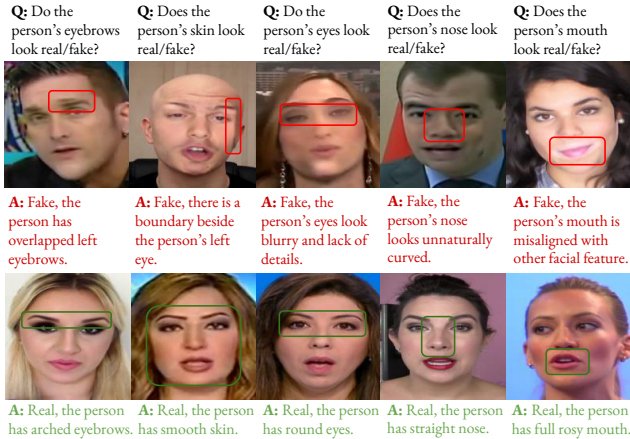


Figure 2. Fine-grained question-answer pairs in DD-VQA Dataset. Red and green fonts show the fake and real answers, respectively.

age. The format of the general question is “Does the person in the image look fake?”. The answers to this question cover the general reasons for authenticity or fakeness. Specifically, the general fakeness factors include “obvious manipulated region”, “incomplete face feature”, “unrealistic texture or lighting”, etc. Conversely, the general reasons for authenticity involve “complete face features”, “face features in good shape, size, and positioning.”, “natural expression”, etc.

Fine-Grained Facial Feature Questions assess the authenticity of individual facial features. There are instances where specific facial components may still exhibit authenticity despite the overall image appearing fake. The detailed facial features include *eyebrows*, *skin*, *eyes*, *nose*, and *mouth*. The format of the fine-grained feature question is “Do the person’s X look real/fake?”, and X is any facial component. We show the corresponding examples in Fig. 2.

The answers to the fake facial components are designed based on their unnatural appearance. We acknowledge that the appearance of individual facial components can greatly differ among individuals, but there are shared common traits and characteristics that can be utilized to identify manipulated images, introduced as follows.

- **Eyebrows.** Humans commonly have a pair of eyebrows with a symmetrical shape, smooth hair, and a dark color. The presence of overlapping, broken and blurred eyebrows can serve as indicators of manipulated images.
- **Skin.** There is no universally “perfect” type of skin; however, generally, common skin should exhibit clarity, an even skin tone, and a smooth texture, especially at lower resolutions. Also, the presence of boundaries, discolored patches, or drastically inconsistent skin color on the face are not characteristic of a real person’s face.
- **Eyes.** Common eyes include the characteristics of symmetry, clarity, expressiveness, an appropriate size, etc. The blurred and asymmetric eyes in the manipulated image can indicate fakeness.

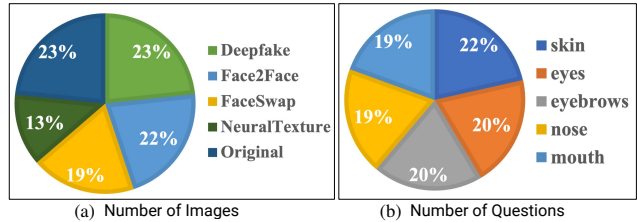


Figure 3. Statistics of the DD-VQA dataset with the respect of the distribution of manipulation method and facial components.

- **Nose.** An ideal nose should be appropriately positioned, with clear and proportionate nostrils in terms of shape and size. However, the unnaturally curved nose or nose without fine lines are obvious fake signs.
- **Mouth.** The mouth in our annotation scheme refers to mouth areas, including lips, teeth and chin. The appearance of inappropriate size and color of these areas could be used to indicate fakeness.

Beyond appearance-related reasons, we also include expression-related reasons, such as “furrowed eyebrows”, “rigid eyes”, and “rigid mouth”, which is also important to deepfake detection. In contrast, if the facial components appear authentic, the answers consist of corresponding descriptive expressions, such as “arched eyebrows”, “round eyes”, “straight nose”, etc.

Besides the above fine-grained facial features, we also consider other features such as haircut, mustache, beard, glass frames and the image’s background. After collecting the annotation of answers for each question, we employ a template-based method to post-process the annotators’ choices and any additional reasons they provide. The template of the answer is “The X looks real/fake because X looks Y”, X represents the entire image or any facial component, and Y denotes the corresponding reason. In cases with multiple reasons, we use commas to combine them as the final answer. Additionally, for general questions, except for collecting the provided general reasons, we randomly select two reasons from the fine-grained answers of the same image as its complementary reasons. This helps to answer general questions more comprehensively.

3.1.2 Statistics of the DD-VQA Dataset

Given the variation in people’s perceptions of authenticity, we gather annotations from three annotators for each image. In the detection aspect of the answer (fake/real), we adopt the majority choice, wherein, we gather annotations when at least two of the annotators are in agreement. Then, we keep all of their provided explanations in the answer. As a result, for each question, up to three answers are collected. Annotators are given the option to skip the question if they are unable to answer. This results in various numbers of question-answers pairs for each image.

On average, we collect approximately 3 to 6 question-

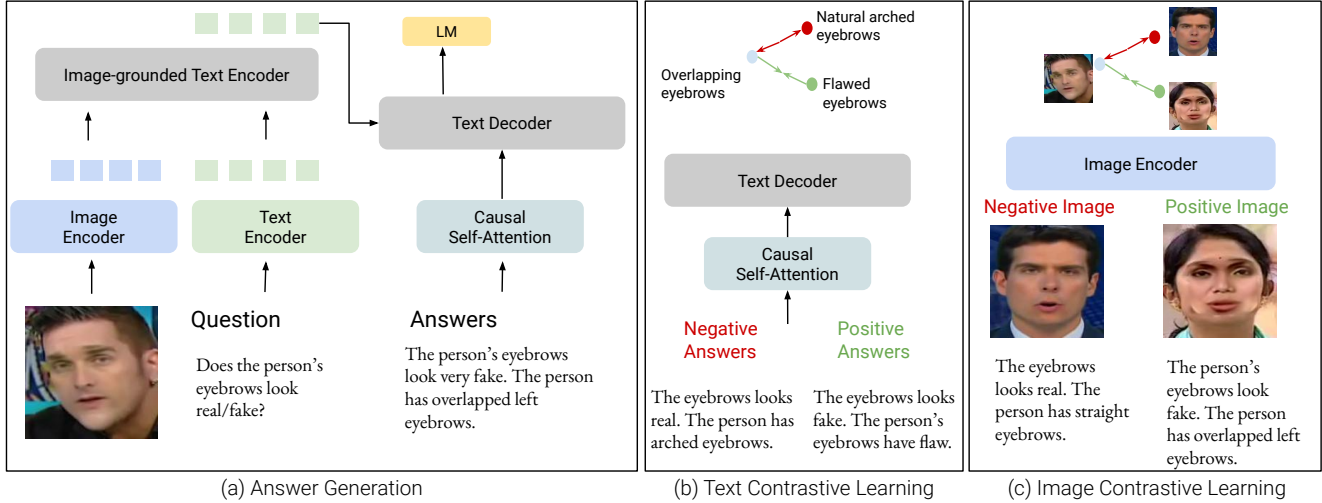


Figure 4. **Model Architecture.** The model takes the image and question as input and generate textual answers in an auto-regressive manner, as shown in (a). To enhance representation learning, we explore two contrastive losses. In (b), we gather negative and positive answers to optimize the text encoder and decoder. In (c), we use answers to filter the negative and positive images to optimize the image encoder.

answer pairs for each image. After gathering all annotations, we remove low-quality annotations according to the following criteria:

1. Absence of answers to all questions for an image.
2. Conflicting annotations where annotators select both “real” and “fake” labels for the same question, which means the annotators are unsure about their decisions.
3. Annotations that are different from the ground-truth detection labels. We also value how people perceive the authenticity of an image. For example, if an image successfully fools the annotators, their answers to the question may not be reliable.

In conclusion, we collect a dataset of 2,968 images and 14,782 question-answer pairs. We provide statistics of the DD-VQA dataset in Fig. 3 from the two perspectives: (1) In Fig. 3 (a), we show the distribution of different manipulated methods. The distribution is quite even while the number of the images manipulated by *NeuralTexture* technique are relatively smaller, indicating this technique relatively fools people more than other manipulation techniques. (2) In Fig. 3 (b), we show the distribution of different facial components in those questions. The result shows an even distribution among different facial components.

3.2. Method

The DD-VQA task generates a textual answer given question and a image with a focus on assessing the authenticity of the image. We adopt BLIP [25] as our backbone, a robust Transformer-based VL model that is pre-trained on noisy web data and bootstraps captions. BLIP is a strong backbone due to its competitive performance across various vision and language tasks, as well as its ease of training. We demonstrate our model architecture in Fig. 4.

3.2.1 Model Architecture

Text Encoder. We formally define question as Q and apply a BERT [10] tokenizer to split the questions to a sequence of tokens, denoted as $Q = \{[CLS], q_1, q_2, \dots, q_l, [SEP]\}$, where l is the length of question tokens. $[CLS]$ and $[SEP]$ are the special tokens. The question is passed through a text encoder, which consists of a multi-layer self-attention block and obtain the text representations, denoted as $X_q = [x_{q1}, x_{q2}, \dots, x_{ql}]$.

Image Encoder. We use a Vision Transformer (ViT) [12] as our image encoder. The image is first divided into m patches, and then encoded as a sequence of embedding with $[CLS]$ token as the global image representations. We define the obtained vision representations from ViT as $I = [i_1, i_2, \dots, i_m]$.

Image-grounded Text Encoder. We apply cross-modal attention layers between the text representations of question X_q and visual representations of image V to inject visual information to the question. We obtain the attended text representation \bar{X}_q as follows,

$$\bar{X}_q = \text{cross_attn}(Q = X_q, K = I, V = I), \quad (1)$$

where Q , K and V are the query, key, and value for attention calculation, respectively.

Text Decoder. Similar to a question, we apply a BERT tokenizer to an answer A to obtain a sequence of answer tokens, denoted as $A = \{[CLS], a_1, a_2, \dots, a_k, [SEP]\}$, where k is the length of tokens. We also acquire text representations of the answer through BERT. However, instead of utilizing self-attention as in the text encoder for question, we employ causal self-attention layers to only attend to the previous tokens instead of all tokens. We represent the text

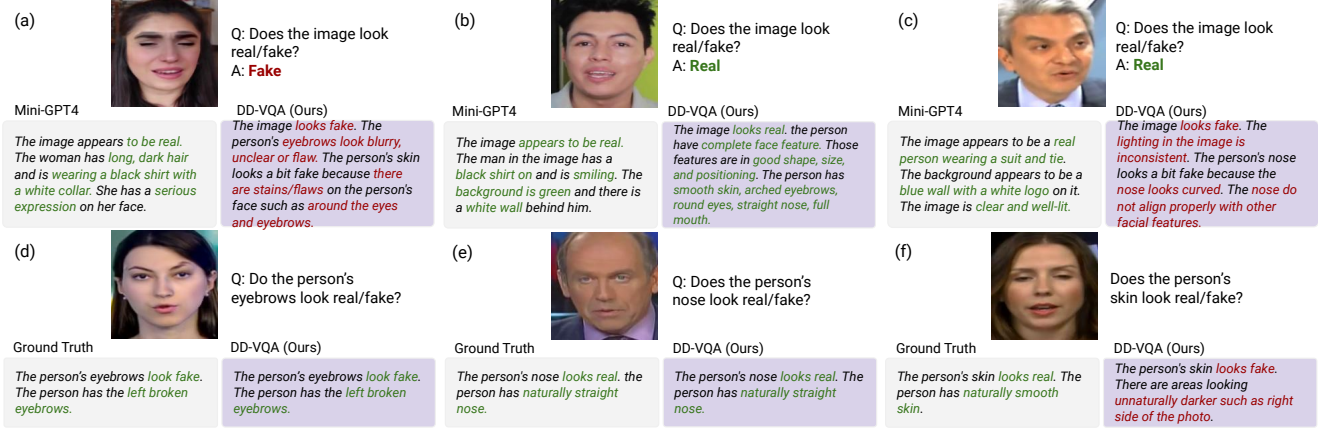


Figure 5. **Qualitative Results.** *MiniGPT-4* [55] vs *DD-VQA (Ours)* in (a)–(c), where (a) and (b) are the successful cases, and (c) is the failure case. *Ground-truth* vs *DD-VQA (Ours)* for fine-grained questions in (d)–(f), where (d) and (e) are successful cases, while (f) is the failure case. The green fronts are the real-related texts and red fronts are the fake-related texts.

representations of the answer as $X_a = [x_{a1}, x_{a2}, \dots, x_{ak}]$. Subsequently, another cross-modal attention layer for decoding the next token is applied between the attended question representation \bar{X}_q and X_a , as follows,

$$\bar{X}_a = \text{cross_attn}(Q = X_a, K = \bar{X}_q, V = \bar{X}_q), \quad (2)$$

where, \bar{X}_a is the attended answer representation given image and question, which is then fed to a Multi-layer Perceptron (MLP) to predict the answer tokens.

3.2.2 Learning Objectives

We use the following objectives to train our model: language modeling to generate answer tokens, text, and image contrastive learning to leverage annotated textual information to enhance the model’s capability to distinguish between real and fake facial components.

Language Modeling aims to generate answer tokens auto-regressively, given a question and an image. Specifically, it is a cross-entropy loss that maximizes the likelihood of the answer tokens conditioned on the previous tokens and the attended question representations, as follows:

$$\mathcal{L}_{LM} = - \sum_{j=1}^k \log p_{\theta}(a_j | a_1, \dots, a_{j-1}, \bar{X}_q), \quad (3)$$

where θ denotes the model’s trainable parameters. There are a maximum of three candidate answers for each question, and we compute the average loss of all answers.

Text Contrastive Learning aims to train the model with different answers given the same images and questions. We filter a negative and a positive answer based on ground-truth answers. The negative answers are obtained by choosing answers on the same facial component but with the opposite detection results. For instance, in Fig. 4 (b), the negative answer is the description of “*real eyebrows*” given the ground-truth “*fake eyebrows*”. The positive answer is randomly

selected from the candidate answers of the current example. We input negative and positive answers to the text encoder and text decoder and use the corresponding representation of the [CLS] token representation from the last layer of the decoder to do text contrastive learning. We denote anchor, positive and negative answer representation as \bar{X}_{aa} , \bar{X}_{ap} and \bar{X}_{an} , respectively. Then, the InfoNCE loss [30] is used for contrastive learning as follows,

$$\mathcal{L}_{\mathcal{T}} = -\log \frac{\exp(\bar{X}_{aa} \cdot \bar{X}_{ap})/\tau}{(\exp(\bar{X}_{aa} \cdot \bar{X}_{ap}) + \exp(\bar{X}_{aa} \cdot \bar{X}_{an}))/\tau}, \quad (4)$$

where τ is the temperature. The aim is to learn the attended text representation that is close to the positive answer but far apart from the negative answer.

Image Contrastive Learning aims to learn the visual representation that can help the model generate correct answers. We train the model with different images given the same question and answer. We filter the positive and negative images based on the answer of the input image. For example, in Fig. 4 (c), when the answer is “*overlapped eyebrows*“, the positive image is the one annotated as “*overlapped eyebrows*” and the negative image is the one annotated as “*natural eyebrows*”. After obtaining positive and negative images, we optimize the image encoder. We use [CLS] token representation from ViT to do image contrastive learning. We represent the anchor, positive and negative image representation as i_a , i_p , and i_n , and calculate losses as follows,

$$\mathcal{L}_{\mathcal{I}} = -\log \frac{\exp(i_a \cdot i_p)/\tau}{(\exp(i_a \cdot i_p) + \exp(i_a \cdot i_n))/\tau} \quad (5)$$

The final objective to train the model is the sum of the three above losses, denoted as:

$$\mathcal{L} = \mathcal{L}_{LM} + \mathcal{L}_{\mathcal{T}} + \mathcal{L}_{\mathcal{I}} \quad (6)$$

| # | Method | Deepfake Detection | | | | Answer Generation | | | | |
|---|----------------------|--------------------|-------------------|----------------------|---------------|-------------------|------------------|--------------------|-------------------|------------------|
| | | Acc \uparrow | Recall \uparrow | Precision \uparrow | F1 \uparrow | BLUE-4 \uparrow | CIDEr \uparrow | ROUGE_L \uparrow | METEOR \uparrow | SPICE \uparrow |
| 1 | BLIP [25] (baseline) | 0.8168 | 0.9596 | 0.7861 | 0.8642 | 0.3569 | 1.8177 | 0.5664 | 0.3301 | 0.6658 |
| 2 | BLIP-T (ours) | 0.8365 | <u>0.9489</u> | 0.8131 | 0.8758 | 0.3714 | 1.8715 | 0.5774 | 0.3349 | 0.6710 |
| 3 | BLIP-I (ours) | <u>0.8487</u> | 0.9448 | <u>0.8298</u> | <u>0.8836</u> | <u>0.3800</u> | <u>1.8931</u> | <u>0.5882</u> | <u>0.3419</u> | <u>0.6788</u> |
| 4 | BLIP-TI (ours) | 0.8749 | 0.9341 | 0.8697 | 0.9007 | 0.4075 | 2.0567 | 0.6085 | 0.3463 | 0.6915 |

Table 2. Experimental Results of DD-VQA on both the performance of deepfake detection and answer generation. Our deepfake detection results are derived from the generated text token rather than a classification result, so we do not provide AUC metrics, a common reporting measure in other deepfake detection methods. BLIP-T: BLIP+text contrastive loss. BLIP-I: BLIP+image contrastive loss. BLIP-TI: BLIP+text+image contrastive loss. We show the best results in bold font and underline the second-best results.

| Method | Acc \uparrow | Recall \uparrow | Precision \uparrow | F1 \uparrow |
|-----------|----------------|-------------------|----------------------|---------------|
| Det. | 0.7978 | 0.9639 | 0.7588 | 0.8492 |
| Det.+Exp. | 0.8168 | 0.9596 | 0.7861 | 0.8642 |

Table 3. Results of BLIP trained on the data with 1) detection and 2) detection and explanation. Det.: Detection, Exp.: Explanation.

4. Experiments

In this section, we report our experimental settings and our quantitative and qualitative results.

4.1. Dataset and Evaluation Metrics

We conduct experiments on the proposed DD-VQA dataset that includes 14, 782 question-answer pairs. Following the FF++ train/test ids, we partition the dataset into training and testing sets, resulting in 13, 559 question-answer pairs for training and 1, 223 for testing. The training dataset contains 2, 726 images, while the test dataset contains 242 images. We evaluate the generated answer on two aspects: the performance of deepfake detection and the quality of generated explanations. To assess detection results, we provide metrics that include Accuracy, Precision, Recall and F1-Score.

We do not follow the conventional deepfake detection model, which typically utilizes the AUC metric. This is because our generated space is whole vocabulary text tokens of BERT rather than limited to binary outputs. In assessing the explanation quality, we use natural language generation metrics such as BLUE-4 [31], CIDEr [50], ROUGE_L [27], METEOR [9], and SPICE [3]. These scores serve to evaluate the similarity between the generated answers and the annotated answers. Please see more details about evaluation metrics are in the Appendix.

4.2. Results on DD-VQA

We fine-tune BLIP on the DD-VQA dataset and provide results for both deepfake detection and the quality answer generation results. Our models effectively capture the answer templates of “The X looks real/fake. The person’s X looks Y”. Additionally, we observe an absence of cases where the detection results conflict with their corresponding explanations. In such a case, we split the generated text into sentences and extract the tokens of “fake” or “real” in the first sentence to assess the deepfake detection performance.

| Method | Acc \uparrow | Recall \uparrow | Precision \uparrow | F1 \uparrow |
|----------|----------------|-------------------|----------------------|---------------|
| Eyebrows | 0.8645 | 0.9189 | 0.8571 | 0.8870 |
| Skin | 0.8899 | 0.9534 | 0.8786 | 0.9145 |
| Eyes | 0.8750 | 0.9224 | 0.8770 | 0.8992 |
| Nose | 0.8800 | 0.9237 | 0.8790 | 0.9008 |
| Mouth | 0.8670 | 0.9459 | 0.8468 | 0.8936 |

Table 4. Deepfake detection performance on fine-grained questions.

| Method | Acc \uparrow | Recall \uparrow | Precision \uparrow | F1 \uparrow |
|---------------------|----------------|-------------------|----------------------|---------------|
| Efficient ViT [8] | 0.6849 | 0.7259 | 0.7538 | 0.7396 |
| Conv. Cross ViT [8] | 0.7763 | 0.7778 | 0.8468 | 0.8108 |
| BLIP-TI (ours) | 0.8719 | 0.9367 | 0.8757 | 0.9052 |

Table 5. Comparison with other Deepfake Detection Models.

We conduct an ablation to assess the impact of our proposed contrastive losses on top of the baseline.

In Table 2 we present our results. Specifically, Row#1 shows the baseline performance. On top of it, we add text contrastive loss, as shown in Row#2, both deepfake detection performance and answer generation quality improve. In Row#3, we present results obtained by training the model with LM and image contrastive loss. The results show that image contrastive loss is more effective than text contrastive loss. The best result in Row#4 is achieved by training the model with all losses, resulting in an improvement of nearly 3% in F1 and 6% in accuracy over the BLIP baseline (Row#1). This indicates the effectiveness of our method in enhancing representation learning for deepfake detection task, based on textual information.

4.3. Ablation Study

Does explanation help in deepfake detection? We conduct an experiment to train BLIP with only deepfake detection, without providing corresponding explanations. Specifically, the answer template for each question is “The X looks real/fake.” The results in Tab 3, indicate that the detection performance is higher when explanations are included. The results also suggest that the incorporation of common-sense knowledge within explanations can improve deepfake detection performance.

Detection performance on fine-grained questions. In Tab. 4, we analyze the model’s performance across different fine-grained questions, and the results indicate that the



Figure 6. Attention heatmap visualization of the baseline BLIP (top) and BLIP-TI (bottom).

model consistently achieves satisfactory detection results for all specific questions. We hypothesize that the reason why the model obtains the best result for the skin question can be the relatively higher number of question-answer pairs related to skin in our dataset, as shown in Fig. 3 (b).

Comparison with ViT-based deepfake detection models.

As our model is a multi-modal Transformer, we compare it with pure ViT Transformer-based deepfake detection models to assess whether adding additional text information contributes to performance improvement. We compare against Efficient ViT [8] and Convolutional Cross ViT [8]. Efficient ViT combines a ViT with a convolutional EfficientNet B0 as the feature extractor. Convolutional Cross ViT builds upon both the Efficient ViT and the multi-scale Transformer, and enable the utilization of larger patches to achieve a broader receptive field. Although, both Efficient ViT and Convolutional Cross ViT use video deepfake datasets (FF++ [35] and DFDC [11]), they extract frames from videos and use images for model training. We evaluate their trained model with images in the DD-VQA dataset and compare them only with our answers from general questions to assess the authenticity of the entire image. The results have been shown in Tab.5. While, convolutional Cross ViT can obtain much better performance on Efficient ViT, however, their results are still significantly below our model, even though both models have been trained on the FF++ dataset.

4.4. Qualitative Study

Qualitative examples. We provide qualitative examples in Fig. 5. We show answers generated by Mini-GPT4 [55], one of the powerful VL pre-trained models, and compare them with our answers for the same question and image. Mini-GPT4 tends to perceive every image as real, offering detailed descriptions of human facial components, clothing, and the background. In contrast, our DD-VQA excels in providing better detection results and accurately explaining the reasons behind the authenticity or fakeness of the image.

Visualization. In Fig. 6, we illustrate an example to visualize the attention heatmap of the last cross-attention layer in the image-grounded encoder. This visualization aims to



Figure 7. Evaluation on Midjourney images given general question to assess authenticity of the image.

assess the model’s ability to identify specific regions given the fine-grained questions. We conduct a comparison between the BLIP baseline and BLIP-TI. The results show that BLIP alone is already capable of roughly identifying the corresponding region, while the incorporation of our contrastive losses enhances the accuracy of localization, such as “eyes” and “mouth” in the example.

Generalization ability. The images in the DD-VQA dataset are generated from CNN-based models. To evaluate our model’s generalization ability, we assess its performance on images generated from diffusion-based models. Specifically, we generate images with human face from Midjourney³ and then evaluate our model’s deepfake detection performance on these images. We finally collected 50 images, and our model successfully recognize 35 as fake. From those examples, the most fake reasons are “skin texture is overly smooth” and “eyes are too rigid”. We provide examples in Fig. 7.

5. Conclusion

This paper proposes a novel task that extends deepfake detection from a conventional binary classification to a VQA task. Our aim is to integrate human common-sense knowledge into deepfake detection in the form of textual explanation. We provide annotated dataset and benchmark for this task. We explore enhancing the baseline model through contrastive learning. Our experiments demonstrate that the inclusion of textual explanations is beneficial for both interpretability and detection performance of the deepfake detection.

Limitations. We acknowledge the following limitations: (1) Our method may be less effective on high-quality deepfake images designed to deceive humans. (2) Our dataset needs more exploration of other deepfake images, such as CGI and diffusion-based images. (3) We have yet to explore the performance with other VL backbone models.

Future Work. We will expand the DD-VQA dataset to a larger scale and explain deepfake images generated from diffusion-based models. We can also apply our method to various modalities for deepfake tasks, such as audio and video, investigating different common-sense formulations.

Ethic Statement. We use publicly available datasets FF++, and discourage any use of our methods for malicious purposes. We commit not to conduct experiments on any images depicting medical deformities.

³<https://www.midjourney.com/>

References

- [1] Harsh Agrawal, Karan Desai, Yufei Wang, Xinlei Chen, Rishabh Jain, Mark Johnson, Dhruv Batra, Devi Parikh, Stefan Lee, and Peter Anderson. Nocaps: Novel object captioning at scale. In *Proceedings of the IEEE/CVF international conference on computer vision*, pages 8948–8957, 2019. **3**
- [2] Jean-Baptiste Alayrac, Jeff Donahue, Pauline Luc, Antoine Miech, Iain Barr, Yana Hasson, Karel Lenc, Arthur Mensch, Katherine Millican, Malcolm Reynolds, et al. Flamingo: a visual language model for few-shot learning. *Advances in Neural Information Processing Systems*, 35:23716–23736, 2022. **2**
- [3] Peter Anderson, Basura Fernando, Mark Johnson, and Stephen Gould. Spice: Semantic propositional image caption evaluation. In *Computer Vision—ECCV 2016: 14th European Conference, Amsterdam, The Netherlands, October 11–14, 2016, Proceedings, Part V 14*, pages 382–398. Springer, 2016. **7, 1**
- [4] Peter Anderson, Qi Wu, Damien Teney, Jake Bruce, Mark Johnson, Niko Sünderhauf, Ian Reid, Stephen Gould, and Anton Van Den Hengel. Vision-and-language navigation: Interpreting visually-grounded navigation instructions in real environments. In *Proceedings of the IEEE conference on computer vision and pattern recognition*, pages 3674–3683, 2018. **3**
- [5] Stanislaw Antol, Aishwarya Agrawal, Jiasen Lu, Margaret Mitchell, Dhruv Batra, C Lawrence Zitnick, and Devi Parikh. Vqa: Visual question answering. In *Proceedings of the IEEE international conference on computer vision*, pages 2425–2433, 2015. **3**
- [6] Weiming Bai, Yufan Liu, Zhipeng Zhang, Bing Li, and Weiming Hu. Aunet: Learning relations between action units for face forgery detection. In *Proceedings of the IEEE/CVF Conference on Computer Vision and Pattern Recognition*, pages 24709–24719, 2023. **1**
- [7] François Chollet. Xception: Deep learning with depthwise separable convolutions. In *Proceedings of the IEEE conference on computer vision and pattern recognition*, pages 1251–1258, 2017. **2**
- [8] Davide Alessandro Coccomini, Nicola Messina, Claudio Genaro, and Fabrizio Falchi. Combining efficientnet and vision transformers for video deepfake detection. In *International conference on image analysis and processing*, pages 219–229. Springer, 2022. **7, 8**
- [9] Michael Denkowski and Alon Lavie. Meteor universal: Language specific translation evaluation for any target language. In *Proceedings of the ninth workshop on statistical machine translation*, pages 376–380, 2014. **7, 1**
- [10] Jacob Devlin, Ming-Wei Chang, Kenton Lee, and Kristina Toutanova. Bert: Pre-training of deep bidirectional transformers for language understanding. *arXiv preprint arXiv:1810.04805*, 2018. **5**
- [11] Brian Dolhansky, Joanna Bitton, Ben Pflaum, Jikuo Lu, Russ Howes, Menglin Wang, and Cristian Canton Ferrer. The deepfake detection challenge (dfdc) dataset. *arXiv preprint arXiv:2006.07397*, 2020. **8**
- [12] Alexey Dosovitskiy, Lucas Beyer, Alexander Kolesnikov, Dirk Weissenborn, Xiaohua Zhai, Thomas Unterthiner, Mostafa Dehghani, Matthias Minderer, Georg Heigold, Sylvain Gelly, et al. An image is worth 16x16 words: Transformers for image recognition at scale. *arXiv preprint arXiv:2010.11929*, 2020. **1, 5**
- [13] Rachel Lea Draelos and Lawrence Carin. Use hirescam instead of grad-cam for faithful explanations of convolutional neural networks. *arXiv preprint arXiv:2011.08891*, 2020. **1**
- [14] Tom Geller. Overcoming the uncanny valley. *IEEE computer graphics and applications*, 28(4):11–17, 2008. **1**
- [15] Ian Goodfellow, Jean Pouget-Abadie, Mehdi Mirza, Bing Xu, David Warde-Farley, Sherjil Ozair, Aaron Courville, and Yoshua Bengio. Generative adversarial networks. *Communications of the ACM*, 63(11):139–144, 2020. **1**
- [16] Yash Goyal, Tejas Khot, Douglas Summers-Stay, Dhruv Batra, and Devi Parikh. Making the v in vqa matter: Elevating the role of image understanding in visual question answering. In *Proceedings of the IEEE conference on computer vision and pattern recognition*, pages 6904–6913, 2017. **3**
- [17] Xiao Guo, Vishal Asnani, Sijia Liu, and Xiaoming Liu. Tracing hyperparameter dependencies for model parsing via learnable graph pooling network. *arXiv preprint arXiv:2312.02224*, 2023. **2**
- [18] Xiao Guo, Xiaohong Liu, Zhiyuan Ren, Steven Grosz, Iacopo Masi, and Xiaoming Liu. Hierarchical fine-grained image forgery detection and localization. In *Proceedings of the IEEE/CVF Conference on Computer Vision and Pattern Recognition*, pages 3155–3165, 2023. **2**
- [19] Ying Guo, Cheng Zhen, and Pengfei Yan. Controllable guide-space for generalizable face forgery detection. In *Proceedings of the IEEE/CVF International Conference on Computer Vision*, pages 20818–20827, 2023. **1**
- [20] Tanmay Gupta and Aniruddha Kembhavi. Visual programming: Compositional visual reasoning without training. In *Proceedings of the IEEE/CVF Conference on Computer Vision and Pattern Recognition*, pages 14953–14962, 2023. **1**
- [21] Jonathan Ho, Ajay Jain, and Pieter Abbeel. Denoising diffusion probabilistic models. *Advances in neural information processing systems*, 33:6840–6851, 2020.
- [22] Tero Karras, Samuli Laine, Miika Aittala, Janne Hellsten, Jaakko Lehtinen, and Timo Aila. Analyzing and improving the image quality of stylegan. In *Proceedings of the IEEE/CVF conference on computer vision and pattern recognition*, pages 8110–8119, 2020. **1**
- [23] Fatima Khalid, Ali Javed, Hafsa Ilyas, Aun Irtaza, et al. Dfgnn: An interpretable and generalized graph neural network for deepfakes detection. *Expert Systems with Applications*, 222:119843, 2023. **2**
- [24] Brenden M Lake, Tomer D Ullman, Joshua B Tenenbaum, and Samuel J Gershman. Building machines that learn and think like people. *Behavioral and brain sciences*, 40:e253, 2017. **1**
- [25] Junnan Li, Dongxu Li, Caiming Xiong, and Steven Hoi. Blip: Bootstrapping language-image pre-training for unified vision-language understanding and generation. In *International Conference on Machine Learning*, pages 12888–12900. PMLR, 2022. **2, 5, 7**

- [26] Lingzhi Li, Jianmin Bao, Ting Zhang, Hao Yang, Dong Chen, Fang Wen, and Baining Guo. Face x-ray for more general face forgery detection. In *Proceedings of the IEEE/CVF conference on computer vision and pattern recognition*, pages 5001–5010, 2020. 2
- [27] Chin-Yew Lin. Rouge: A package for automatic evaluation of summaries. In *Text summarization branches out*, pages 74–81, 2004. 7, 1
- [28] Ilya Loshchilov and Frank Hutter. Decoupled weight decay regularization. *arXiv preprint arXiv:1711.05101*, 2017. 1
- [29] Yisroel Mirsky and Wenke Lee. The creation and detection of deepfakes: A survey. *ACM Computing Surveys (CSUR)*, 54(1):1–41, 2021. 1, 3
- [30] Aaron van den Oord, Yazhe Li, and Oriol Vinyals. Representation learning with contrastive predictive coding. *arXiv preprint arXiv:1807.03748*, 2018. 6
- [31] Kishore Papineni, Salim Roukos, Todd Ward, and Wei-Jing Zhu. Bleu: a method for automatic evaluation of machine translation. In *Proceedings of the 40th annual meeting of the Association for Computational Linguistics*, pages 311–318, 2002. 7, 1
- [32] Adam Paszke, Sam Gross, Francisco Massa, Adam Lerer, James Bradbury, Gregory Chanan, Trevor Killeen, Zeming Lin, Natalia Gimelshein, Luca Antiga, et al. Pytorch: An imperative style, high-performance deep learning library. *Advances in neural information processing systems*, 32, 2019. 1
- [33] Aditya Ramesh, Prafulla Dhariwal, Alex Nichol, Casey Chu, and Mark Chen. Hierarchical text-conditional image generation with clip latents. *arXiv preprint arXiv:2204.06125*, 1(2): 3, 2022. 1
- [34] Jonas Ricker, Simon Damm, Thorsten Holz, and Asja Fischer. Towards the detection of diffusion model deepfakes. *arXiv preprint arXiv:2210.14571*, 2022. 1
- [35] Andreas Rossler, Davide Cozzolino, Luisa Verdoliva, Christian Riess, Justus Thies, and Matthias Nießner. Faceforensics++: Learning to detect manipulated facial images. In *Proceedings of the IEEE/CVF international conference on computer vision*, pages 1–11, 2019. 2, 3, 8
- [36] Chitwan Saharia, William Chan, Saurabh Saxena, Lala Li, Jay Whang, Emily L Denton, Kamyar Ghasemipour, Raphael Gontijo Lopes, Burcu Karagol Ayan, Tim Salimans, et al. Photorealistic text-to-image diffusion models with deep language understanding. *Advances in Neural Information Processing Systems*, 35:36479–36494, 2022. 1
- [37] Niloufar Salehi, Lilly C Irani, Michael S Bernstein, Ali Alkhatib, Eva Ogbe, Kristy Milland, and Clickhappier. We are dynamo: Overcoming stalling and friction in collective action for crowd workers. In *Proceedings of the 33rd annual ACM conference on human factors in computing systems*, pages 1621–1630, 2015. 1
- [38] Dustin Schwenk, Apoorv Khandelwal, Christopher Clark, Kenneth Marino, and Roozbeh Mottaghi. A-okvqa: A benchmark for visual question answering using world knowledge. In *European Conference on Computer Vision*, pages 146–162. Springer, 2022. 3
- [39] Ramprasaath R Selvaraju, Michael Cogswell, Abhishek Das, Ramakrishna Vedantam, Devi Parikh, and Dhruv Batra. Grad-cam: Visual explanations from deep networks via gradient-based localization. In *Proceedings of the IEEE international conference on computer vision*, pages 618–626, 2017. 1, 2
- [40] Kaede Shiohara and Toshihiko Yamasaki. Detecting deepfakes with self-blended images. In *Proceedings of the IEEE/CVF Conference on Computer Vision and Pattern Recognition*, pages 18720–18729, 2022. 1
- [41] Karen Simonyan, Andrea Vedaldi, and Andrew Zisserman. Visualising image classification models and saliency maps. *Deep Inside Convolutional Networks*, 2, 2014. 2
- [42] Ke Sun, Shen Chen, Taiping Yao, Xiaoshuai Sun, Shouhong Ding, and Rongrong Ji. Towards general visual-linguistic face forgery detection. *arXiv preprint arXiv:2307.16545*, 2023. 2
- [43] Mukund Sundararajan, Ankur Taly, and Qiqi Yan. Axiomatic attribution for deep networks. In *International conference on machine learning*, pages 3319–3328. PMLR, 2017. 2
- [44] Mingxing Tan and Quoc Le. Efficientnet: Rethinking model scaling for convolutional neural networks. In *International conference on machine learning*, pages 6105–6114. PMLR, 2019. 2
- [45] Ruben Tolosana, Ruben Vera-Rodriguez, Julian Fierrez, Aythami Morales, and Javier Ortega-Garcia. Deepfakes and beyond: A survey of face manipulation and fake detection. *Information Fusion*, 64:131–148, 2020. 1
- [46] Loc Trinh, Michael Tsang, Sirisha Rambhatla, and Yan Liu. Interpretable and trustworthy deepfake detection via dynamic prototypes. In *Proceedings of the IEEE/CVF winter conference on applications of computer vision*, pages 1973–1983, 2021. 2
- [47] Trieu H Trinh and Quoc V Le. A simple method for commonsense reasoning. *arXiv preprint arXiv:1806.02847*, 2018. 1
- [48] William Turton and Andrew Martin. How deepfakes make disinformation more real than ever. *Bloomberg News*, 2020. 1
- [49] Cristian Vaccari and Andrew Chadwick. Deepfakes and disinformation: Exploring the impact of synthetic political video on deception, uncertainty, and trust in news. *Social Media+ Society*, 6(1):2056305120903408, 2020. 1
- [50] Ramakrishna Vedantam, C Lawrence Zitnick, and Devi Parikh. Cider: Consensus-based image description evaluation. In *Proceedings of the IEEE conference on computer vision and pattern recognition*, pages 4566–4575, 2015. 7, 1
- [51] Oriol Vinyals, Alexander Toshev, Samy Bengio, and Dumitru Erhan. Show and tell: Lessons learned from the 2015 mscoco image captioning challenge. *IEEE transactions on pattern analysis and machine intelligence*, 39(4):652–663, 2016. 3
- [52] Yue Zhang and Parisa Kordjamshidi. Explicit object relation alignment for vision and language navigation. In *Proceedings of the 60th Annual Meeting of the Association for Computational Linguistics: Student Research Workshop*, pages 322–331, 2022. 3
- [53] Yue Zhang and Parisa Kordjamshidi. Lovis: Learning orientation and visual signals for vision and language navigation. *arXiv preprint arXiv:2209.12723*, 2022.

- [54] Yue Zhang and Parisa Kordjamshidi. Vln-trans: Translator for the vision and language navigation agent. *arXiv preprint arXiv:2302.09230*, 2023. [3](#)
- [55] Deyao Zhu, Jun Chen, Xiaoqian Shen, Xiang Li, and Mohamed Elhoseiny. Minigt-4: Enhancing vision-language understanding with advanced large language models. *arXiv preprint arXiv:2304.10592*, 2023. [2](#), [6](#), [8](#)

Common Sense Reasoning for Deepfake Detection

Supplementary Material

6. DD-VQA Dataset Annotations

Annotation Tools. Annotations for DD-VQA are collected entirely by crowd workers from Amazon Mechanical Turk (AMT)⁴. The dataset is collected over the course of 3 months and 3 iterations of updating annotation schemes. Approximate 9000 Human Intelligence Tasks (HITs) are launched on AMT, where each HIT involves 3-6 questions, answers, and the corresponding images. Each HIT was designed such that workers manage to earn anywhere between \$6-\$8 per hour, which follows ethical research standards on AMT [37].

Fakeness Annotations. From Tab. 11-Tab.11, we present examples of fine-grained fake facial features and the corresponding descriptions in our dataset. We provide the annotators with fine-grained feature options and use templates to comprise the description with our templates. Some fakenesses require the annotators to provide the corresponding area, for example, “*left or right eyebrows*”. Also, for the question of which area looks unnatural brighter/darker, the answers need to include the corresponding facial areas, such as “*left/right cheeks*”, “*beside the left/right eyes*”, “*around nose*”, etc.

Challenging Annotation Cases. In Fig 9, we provide examples where at least two annotators mistakenly perceive manipulated images as real. Such cases are excluded when annotators provide inaccurate labels, as effective deception of humans requires the human face in the image to adhere to common-sense knowledge.

Uncertainty of Fakeness. There are cases where annotators express uncertainty regarding the authenticity of the image. To capture this ambiguity, we offer annotators a fakeness rating scale ranging from 0 to 5, where 0 and 1 indicate authenticity, 2 and 3 means a slight degree of fakeness, and 4 and 5 represent a high degree of fakeness. The corresponding descriptions are “real”, “a bit fake”, and “very fake”. Annotating the uncertainty of fakeness helps the model in simulating human’s perception of fakeness, thereby enhancing its ability to generate explanations that align more accurately with human judgment.

7. Experiment Setup

Metrics We mainly use image-caption-based metrics to evaluate the quality of the generated text, as follows.

- **BLEU-4** [31] is used to evaluate the precision of the match between the generated text and reference text based on 4-grams.

⁴<https://www.mturk.com/>

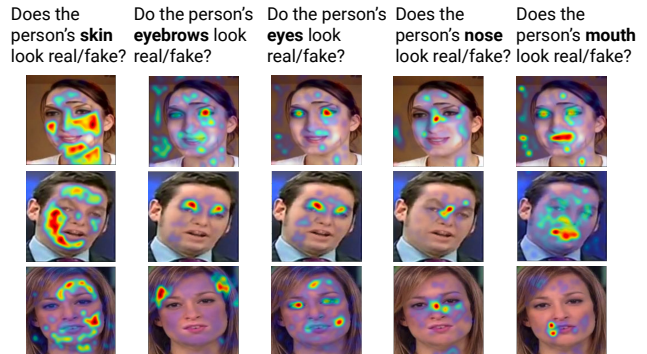


Figure 8. Additional attention heatmap visualization of BLIP-TI.



Figure 9. Challenging cases where annotators provide incorrect labels.

- **CIDEr** [50] measures the consensus between the generated text and the referenced text, considering both word and grammar similarity and the alignment in terms of meaning and content.
- **Rouge_L** [27] evaluates the Longest Common Subsequence (LCS) of words between the generated text and the referenced text. Using LCS does not require consecutive matches but in-sequence matches reflecting sentence-level word order.
- **METEOR** [9] considers precision, recall, stemming, synonymy, and word order. It employs a unigram-based matching approach but extends it with additional semantic features.
- **SPICE** [3] evaluates how well a generated text can capture the specific entities present in the image, emphasizing precision, recall, and diversity.

Implementation Details. Our models are implemented in PyTorch [32]. We use BLIP-base weights as our initial pre-training weights and the image transformer is ViT-B/16. We fine-tune BLIP on our DD-VQA dataset. We conduct 300 epochs using 3 NVIDIA RTX GPUs (72 hours), with a batch size of 8 and a learning rate of $2e - 5$. We use AdamW [28] as the optimizer with weight decay of 0.05. During inference, the max generated token is set as 50.

8. More Qualitative Examples

Visualization We present additional visualization examples in Fig.8 generated by our best model BLIP-TI. The

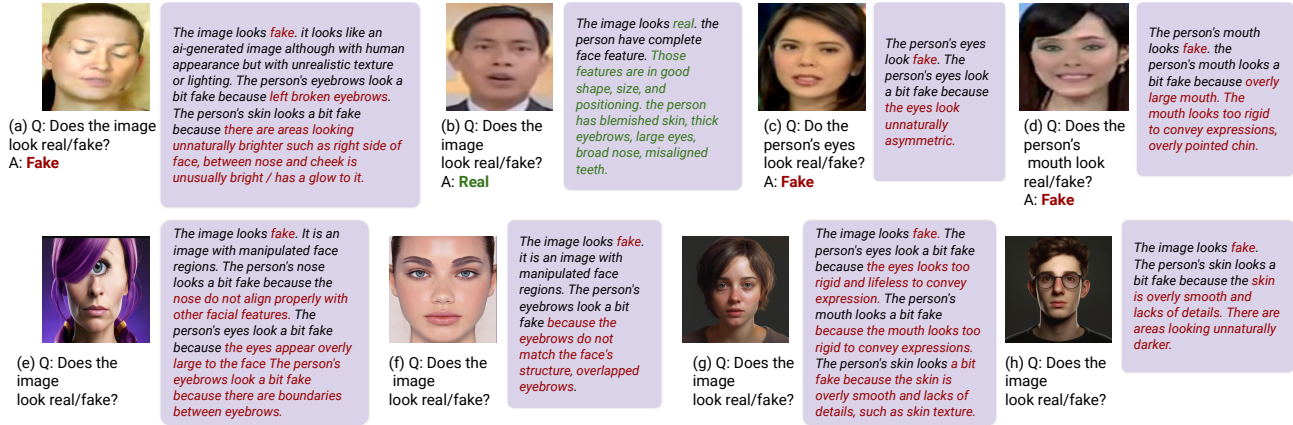


Figure 10. **Additional Qualitative Examples** (a)-(d) are images from FF++. (e) is a cartoon image; (f) is a Photoshop images showing overlapped eyebrows. (g) and (h) are images from Midjourney.

| Fine-grained Features | Images | Descriptions |
|---------------------------|--------|--|
| Overlapped eyebrows | | The person's eyebrows look fake. The person's eyebrows look very fake because the person has left overlapped eyebrow and right overlapped eyebrow. |
| Broken eyebrows | | The person's eyebrows look fake. The person's eyebrows look very fake because the person has broken left eyebrow. |
| Blurry eyebrows | | The person's eyebrows look fake. The person's eyebrows look very fake because the eyebrows look blurry and unclear. |
| Boundary between eyebrows | | The person's eyebrows look fake. The person's eyebrows look fake because there is a boundary between the person's eyebrows. |

Table 6. Fake Eyebrows Features.

model is trained with both language modeling loss and our designed contrastive losses. These example demonstrates that the highlighted attention areas predominantly align with facial components mentioned in the question. We employ GradCam [39] visualization technique to show the alignments between textual tokens and the the highlight area in

the image.

Qualitative Examples We provide additional qualitative examples in Fig. 10. We extend our testing beyond the FF++ dataset. We evaluate our model on diverse images, including cartoon images, Photoshop images, and images generated using a diffusion model. These examples show our model

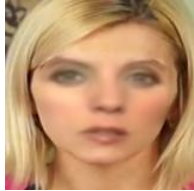


| Fine-grained Features | Images | Descriptions |
|---------------------------|---|---|
| Blurry eyes |  | The person's eyes look fake. The person's eyes look fake because the eyes look blurry and unclear. |
| Unnatural asymmetric eyes |  | The person's eyes look fake. The person's eyes look fake because the person has unnatural asymmetric eyes. |
| Rigid Eyes |  | The person's eyes look fake. The person's eyes look fake because the person's eyes are too rigid to convey expressions. |

Table 7. Fake Eyes Features.

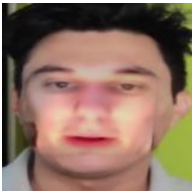
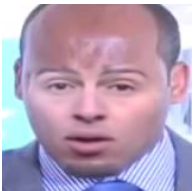

| Fine-grained Features | Images | Descriptions |
|-------------------------|---|---|
| Boundaries |  | The person's skin looks fake. The person's skin looks very fake because there are boundaries on the person's face such as boundary on the person's left and right cheeks. |
| Inconsistent skin color |  | The person's skin looks fake. The person's skin looks very fake because the person has inconsistent skin color. |
| Discolored patches |  | The person's skin looks fake. The person's skin looks very fake because there is a discolored path on the person's forehead. |

Table 8. Fake Skin Features.

can capture common-sense knowledge of human facial feature well. For instance, the cartoon image of Fig. 10 (e), our model can capture the patten of “*over large eyes*”. Also, we manipulate a real image to put another pair of eyebrows on the top of the original eyebrows, as shown in Fig. 10 (f), and our model still can capture the fakeness of “*overlapped eye-*

brows”. For images from Midjourney (Fig. 10 (g) and (h)), our model can capture the fakeness of “*rigid eyes and mouth*”.

DD-VQA User Interface We provide our User interfae in Fig. 11. Users can input questions and our model generate the corresponding answers.



| Fine-grained Features | Images | Descriptions |
|-------------------------|---|---|
| Unnaturally curved nose |  | The person's nose looks fake. The person's nose looks unnaturally curved. |
| nose lacks of details |  | The person's nose looks fake. The person's nose looks very fake because the nose lacks of pores and fine lines. |

Table 9. Fake Nose Features.


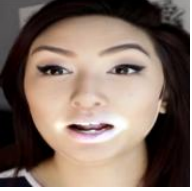

| Fine-grained Features | Images | Descriptions |
|---------------------------------|---|--|
| Blurry Mouth |  | The person's mouth area looks fake. The person's mouth looks blurry and unclear. |
| Mouth with unnatural color |  | The person's mouth area looks fake. The person's mouth shows an unnatural white color. |
| unnatural coloring/blurry teeth |  | The person's mouth area looks fake. The person's teeth look misaligned with the rest of the mouth. The person's teeth look unnatural coloring. |

Table 10. Fake Mouth Features.




| Fine-grained Features | Images | Descriptions |
|----------------------------|---|---|
| Incomplete facial features |  | The image looks fake because the person has incomplete facial features. |
| Unclear eyeglass frame |  | The image looks fake because the person's eyeglass frame looks unclear. |
| Mustache |  | The image looks fake because the person's mustache does not align with other facial features. |

Table 11. General Fake Features.

This is the demo of Deepfake-VQA. Upload your images and ask questions!

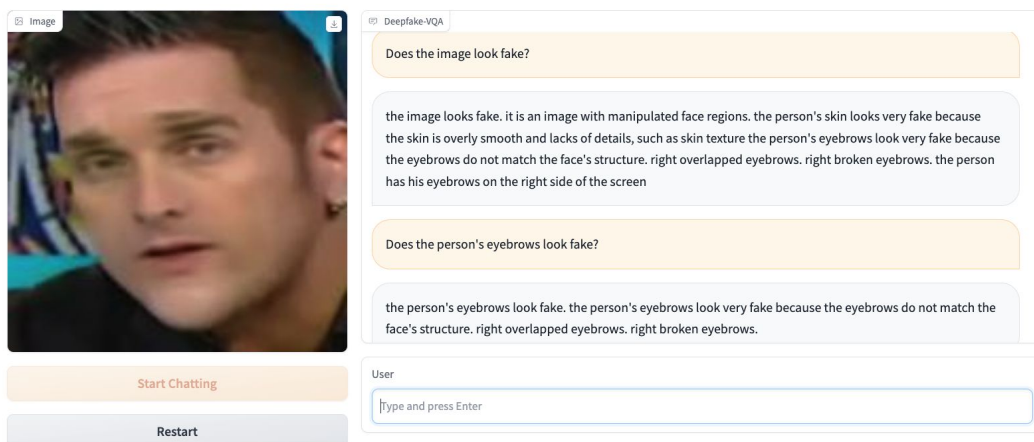


Figure 11. User Interface of the DD-VQA.